Inorg. Chem. **2006**, *45*, 51–58

Electronic Energy-Transfer Rate Constants for Geometrical Isomers of a Bichromophoric Macrocyclic Complex

Evan G. Moore,*,† Paul V. Bernhardt,† Mark J. Riley,† and Trevor A. Smith‡

Department of Chemistry, School of Molecular and Microbial Science, University of Queensland, Brisbane 4072, Australia, and Photophysics Laboratory, School of Chemistry, University of Melbourne, Parkville 3010, Australia

Received March 17, 2005

The rate of electronic energy transfer (EET) between a naphthalene donor and an anthracene acceptor in $[ZnL^3](ClO_4)_2$ and $[ZnL^4](ClO_4)_2$ was determined by time-resolved fluorescence measurements, where L^3 and L^4 are the geometrical isomers of 6-[(anthracen-9-ylmethyl)amino]-*trans*-6,13-dimethyl-1,4,8,11-tetraazacyclotetradecane-13-amine (L^2), substituted with either a naphthalen-1-ylmethyl or naphthalen-2-ylmethyl donor, respectively. The energy-transfer rate constant, k_{EET}, was determined to be $(0.92 \pm 0.02) \times 10^9\ s^{-1}$ for the naphthalen-1-ylmethyl-substituted isomer, while that for the naphthalen-2-ylmethyl-substituted isomer is somewhat faster, with $k_{EET} = (1.31 \pm 0.01) \times 10^9\ s^{-1}$. The solid-state structure of $[ZnL^3Cl]ClO_4$ has been determined, and using molecular modeling calculations, the likely distributions of solution conformations in CH_3CN have been evaluated for both complexes. The calculated conformational distributions in the common *trans*-III N-based isomeric form gave Förster EET rate constants that account for the differences observed and are in excellent agreement with the experimental values. It is shown that the full range of conformers must be considered to accurately reproduce the observed EET kinetics.

Introduction

With a wide variety of applications in diverse areas including light harvesting,[1,2] artificial photosynthesis,[3,4] and polymer photophysics[5] and as components of molecular devices (e.g., polymeric light-emitting diodes, LEDs),[6] excited-state deactivation via electronic excitation (or energy) transfer (EET) and the underlying mechanism of this nonradiative deactivation pathway is of significant interest. Naphthalene and anthracene have proven to be versatile aromatic chromophores notably exploited in order to study these interactions. Compounds that displayed steady-state evidence of intramolecular EET between these chromophores across an alkyl linker were first reported by Schnepp and Levy,[7] and have been subsequently investigated using time-resolved spectroscopy in solution,[8,9] in supersonic jet expansions,[10] and in stretched polymer films[9,11] in order to elucidate the mechanism responsible for the observed EET. Scholes et al.[12] similarly utilized these two chromophores in an investigation of the "through-bond" exchange interaction for a rigidly linked bis(norbornyl)bichromophore, which can mediate EET via orbital overlapping of the bridge with donor and acceptor orbitals. The asymmetrically disubstituted bichromophores shown in Chart 1 are the first examples of systems where the naphthalene and anthracene chromophores have been covalently appended to a tetraaza macrocycle. As such, they are a novel class of compounds that allow a further examination of the role of the linker in determining inter-

* To whom correspondence should be addressed. E-mail: EGMoore@lbl.gov. Current address: Lawrence Berkeley National Laboratory, 1 Cyclotron Road, Mail Stop 70A1150, Berkeley, CA 94720.
† University of Queensland.
‡ University of Melbourne.

(1) Adronov, A.; Frechet, J. M. J. *Chem. Commun.* **2000**, 1701.
(2) Miller, M. A.; Lammi, R. K.; Prathapan, S.; Holten, D.; Lindsey, J. S. *J. Org. Chem.* **2000**, *65*, 6634.
(3) Harriman, A. *Photochemistry* **1998**, *29*, 425.
(4) Gust, D.; Moore, T. A. *Photosynth. React. Cent.* **1993**, *2*, 419.
(5) Adronov, A.; Robello, D. R.; Frechet, J. M. J. *J. Polym. Sci., Part A: Polym. Chem.* **2001**, *39*, 1366.
(6) Pei, J.; Liu, X.-L.; Yu, W.-L.; Lai, Y.-H.; Niu, Y.-H.; Cao, Y. *Macromolecules* **2002**, *35*, 7274.
(7) Schnepp, O.; Levy, M. *J. Am. Chem. Soc.* **1962**, *84*, 172.
(8) Nishimura, Y.; Yasuda, A.; Speiser, S.; Yamazaki, I. *Chem. Phys. Lett.* **2000**, *323*, 117.
(9) Speiser, S.; Hasegawa, M.; Enomoto, S.; Hoshi, T.; Igarashi, K.; Nishimura, Y.; Yasuda, A.; Yamazaki, T.; Yamazaki, I. *J. Lumin.* **2003**, *102−103*, 278.
(10) Wang, X.; Levy, D. H.; Rubin, M. B.; Speiser, S. *J. Phys. Chem. A* **2000**, *104*, 6558.
(11) Hasegawa, M.; Enomoto, S.; Hoshi, T.; Igarashi, K.; Yamazaki, T.; Nishimura, Y.; Speiser, S.; Yamazaki, I. *J. Phys. Chem. B* **2002**, *106*, 4925.
(12) Scholes, G. D.; Ghiggino, K. P.; Oliver, A. M.; Paddon-Row, M. N. *J. Phys. Chem.* **1993**, *97*, 11871.

10.1021/ic050396l CCC: $33.50
Published on Web 12/09/2005

Chart 1. Ligands Discussed in This Paper

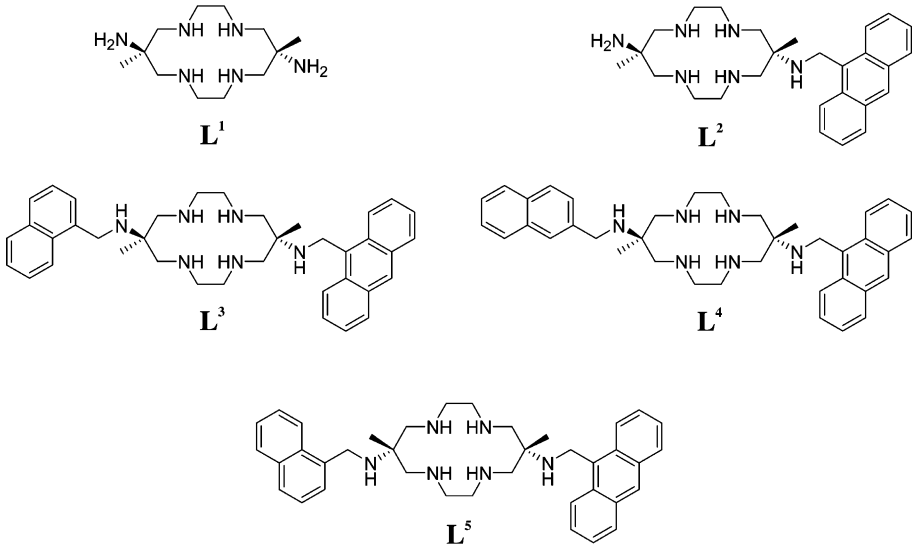

chromophore separation, rigidity, and promotion of intramolecular energy transfer.

For an intramolecular EET process, the general expression for excitation transfer may be written as

$$\mathrm{D^*{-}L{-}A} \xrightarrow{k_{EET}} \mathrm{D{-}L{-}A^*} \qquad (1)$$

where D and A represent the donor and acceptor chromophores, respectively, and L denotes the linker, which either can be inert or may act to facilitate the EET process. Classically, the overall rate constant, k_{EET}, can be attributed to the sum of both a Coulombic (approximated to the dipole−dipole case) and exchange contribution, expressions for which have been provided by Förster[13] and Dexter,[14] respectively. In addition, it has been shown,[12,15] both theoretically and experimentally, that additional relayed and through-bond mechanisms exist that may facilitate electronic coupling (μ_{total}) between donor and acceptor chromophores and hence enhance the rate of energy transfer.

$$\mu_{total} = \mu_{Coul} + \mu_{Exch} + \mu_{rel} + \mu_{tb} \qquad (2)$$

In connection with our studies of the linker's influence on intramolecular EET kinetics, we recently reported the outcome of time-resolved fluorescence studies for EET between the naphthalen-1-ylmethyl and anthracen-9-ylmethyl chromophores appended covalently to the cis and trans isomers of the parent L^1 macrocycle (Chart 1; L^5 and L^3, respectively) in complex with Zn(II).[16] In that case, the observed EET rate constants were in agreement with those predicted using the Förster formulation, accounting for the conformational flexibility of the appended groups. The observed 2-fold increase in k_{EET} between $[ZnL^5]^{2+}$ and $[ZnL^3]^{2+}$ was attributed to differences in the preferred coordination geometry of the macrocycle, which adopts the *trans*-I N-based isomeric form in the former case compared to the more common *trans*-III form for the latter. Herein, we report the influence of utilizing the corresponding geometrical isomer of the donor chromophore, namely, a naphthalen-2-ylmethyl moiety, appended to the trans form of the macrocyclic ligand (Chart 1; L^4). As a compliment, the kinetics of the EET behavior for the $[ZnL^3]^{2+}$ system were reinvestigated under identical conditions, and additional results from a recent structural characterization of this complex are reported.

Experimental Section

Synthesis. The parent macrocycle, *trans*-6,13-dimethyl-1,4,8,-11-tetraazacyclotetradecane-6,13-diamine hexahydrochloride, $L^1 \cdot 6HCl$, was prepared according to a previously reported method[17] and was converted to its free base form by a literature procedure.[18] The syntheses of L^2 and L^3 have similarly been reported elsewhere.[19,20] L^4 was prepared with only slight modifications to the published procedure[20] as outlined below. Corresponding Zn(II) complexes of all ligands were generated in situ by titration with ~1.1 equiv of $Zn(ClO_4)_2 \cdot 6H_2O$. Unless otherwise stated, all other reagents were obtained commercially and used without further purification.

6-[(Anthracen-9-ylmethyl)amino]-*trans*-6,13-dimethyl-13-[(naphthalen-2-ylmethyl)amino]-1,4,8,11-tetraazacyclotetradecane (L^4). L^1 (0.52 g, 2.0 mmol) was dissolved in an $EtOH/H_2O$ mixture [9:1 (v/v), 200 mL], and HCl (1 M) was added until the pH of the resulting clear solution was ca. 5.5. $Na[CN(BH_3)]$ (0.38 g, 6.0 mmol) was added, and the pH was readjusted to 5.5 with NaOH (1 M). Naphthalene-2-carbaldehyde (0.31 g, 2.0 mmol) was added, and the resulting solution was stirred at room temperature for ca. 2 h while the pH was maintained at ca. 5.5 by the addition of aliquots of HCl (1 M) as required. This solution was left to stir overnight, and a precipitate of the symmetrically disubstituted 6,13-bis[(naphthalen-2-ylmethyl)amino]-*trans*-6,13-dimeth-

(13) Förster, T. *Discuss. Faraday Soc.* **1959**, *No. 27*, 7.
(14) Dexter, D. L. *J. Chem. Phys.* **1953**, *21*, 836.
(15) Craig, D. P.; Thirunamachandran, T. *Chem. Phys.* **1989**, *135*, 37.
(16) Moore, E. G.; Bernhardt, P. V.; Pigliucci, A.; Riley, M. J.; Vauthey, E. *J. Phys. Chem. A* **2003**, *107*, 8396.
(17) Bernhardt, P. V.; Lawrance, G. A.; Hambley, T. W. *J. Chem. Soc., Dalton Trans.* **1989**, 1059.
(18) Beer, P. D.; Bernhardt, P. V. *J. Chem. Soc., Dalton Trans.* **2001**, 1428.
(19) Bernhardt, P. V.; Flanagan, B. M.; Riley, M. J. *J. Chem. Soc., Dalton Trans.* **1999**, 3579.
(20) Bernhardt, P. V.; Moore, E. G.; Riley, M. J. *Inorg. Chem.* **2002**, *41*, 3025.

yl-1,4,8,11-tetraazacyclotetradecane, as the bis(cyanoborohydride salt), was collected by vacuum filtration (0.13 g, 0.21 mmol, 10.5%). Excess EtOH was removed from the filtrate at reduced pressure, and H_2O (200 mL) was added. This solution was then made alkaline (pH > 12) by the addition of NaOH (5 M), was extracted with CH_2Cl_2 (3 × 75 mL) and the organic layer was kept and dried over anhydrous Na_2SO. Removal of the solvent at reduced pressure gave the monosubstituted naphthylmethyl intermediate as an oil (0.60 g, 1.51 mmol, 75.3%), with reduced naphthalen-2-ylmethanol present as a contaminant, as confirmed by ^1H and ^{13}C NMR. This oil was redissolved in an EtOH/H_2O mixture [9:1 (v/v), 200 mL], and HCl (1 M) was added until the pH of the resulting clear solution was ca. 6.3. Na[CN(BH_3)] (0.38 g, 6.0 mmol) was added, and the pH was readjusted to 6.3 with HCl (1 M). Anthracene-9-carbaldehyde (0.31 g, 2.0 mmol) was dissolved separately in EtOH (50 mL)

then added, and the resulting solution was stirred at room temperature for ca. 2 h while maintaining the pH at ca. 6.3 by the addition of aliquots of HCl (1 M) as required. This solution was then stirred overnight to give a precipitate of the product as the cyanoborohydride salt $[H_2L^4][(CN)BH_3]_2$, which was collected by vacuum filtration. This solid was suspended in H_2O (200 mL), and NaOH (3 M, 50 mL) was added. The resulting suspension was extracted with CH_2Cl_2 (3 × 75 mL) and dried over anhydrous Na_2SO_4, and removal of the solvent at reduced pressure gave the desired product as an oil. This was redissolved in a warm CH_3CN/CH_2Cl_2 solvent mixture [1:1 (v/v), 100 mL], and the solvent was reduced in volume to give the ligand as a powdery pale yellow solid (0.49 g, 42.1%). Elem Anal. Calcd for $C_{38}H_{48}N_6 \cdot 0.5H_2O$: C, 76.34; H, 8.26; N, 14.06. Found: C, 76.39; H, 8.44; N, 13.92. ^1H NMR ($CDCl_3$): δ 1.14 (s, 3H, CH_3), 1.40 (s, 3H, CH_3), 2.1 (s br, 6H, NH), 2.5−2.9 (m, 16H, CH_2 macrocyclic), 3.89 (s, 2H, N−CH_2−2′-Nap), 4.64 (s, 2H, N−CH_2−Anth), 7.4−7.5 (m, 8H), 7.78−7.81 (m, 3H), 7.97 (d, 2H), 8.37 (s, 1H), 8.42 (d, 2H) ppm. ^{13}C NMR ($CDCl_3$): δ 23.1, 23.2, 38.1, 46.4, 48.7, 48.9, 55.3, 55.8, 57.6, 57.8, 124.5, 124.9, 125.4, 125.8, 125.9, 126.3, 126.9, 127.0, 127.62, 127.65, 127.9, 129.0, 130.4, 131.7, 132.2, 132.6, and 139.0 ppm.

Physical Methods. NMR spectra were measured at 400.13 (^1H) and 100.62 MHz (^{13}C) on a Bruker AV400 spectrometer using CD_3CN as the solvent and referenced to the residual solvent peak. Electronic absorption spectra were measured on a Perkin-Elmer Lambda 40 spectrophotometer using quartz cells. Steady-state emission and excitation spectra were collected on a Perkin-Elmer LS-50B spectrofluorimeter. Samples were purged with N_2 prior to measurements, and cutoff filters were employed to avoid detection of higher order excitation light. Time-resolved fluorescence measurements were performed by time-correlated single-photon counting using an experimental setup similar to that previously described,[21] with two different light sources. An excitation wavelength of 285 nm was achieved using the frequency-doubled output of a cavity-dumped jet stream dye laser (Spectra-Physics model 3500) pumped synchronously by a mode-locked Ar^+ laser (Spectra-Physics model 2030). Rhodamine 6G was used as the dye with the output set to 570 nm using a three-plate birefringent filter. The laser pulse repetition rate was reduced to 4 MHz through intracavity dumping and frequency-doubled in an angle-tuned KDP nonlinear crystal providing excitation pulses of ∼5 ps. Excitation at 390 nm was performed using the output of a Kerr lens mode-locked Ti:sapphire laser (Coherent, Mira 900f) pumped by a continuous-wave Ar^+ laser (Coherent, Innova 400) as the light source. The repetition rate of the 130-fs-duration pulses from the Ti:sapphire laser was reduced to 4 MHz with a home-built pulse picker based on a TeO_2 Bragg cell and CAMAC driver, and the pulses were subsequently frequency-doubled in a BBO nonlinear crystal. The full width at half-maximum of the instrument response function (IRF) for this setup was less than 200 ps. Solution concentrations were $\sim 10^{-5}$ M in an analyte, which, if necessary, were further diluted to maintain an optical density of no more than 0.1 at the excitation wavelength, and samples were degassed thoroughly by purging with N_2 prior to each measurement. Observed fluorescence time profiles were analyzed by iterative reconvolution with the measured IRFs using a nonlinear least-squares fitting procedure based on the Marquardt−Levenberg algorithm using a commercially available software package (Picoquant, FluoFit v3.1.0). The goodness of fit was assessed by minimizing the reduced χ^2 function and a visual inspection of the weighted residuals. Support-plane error analysis was performed with a 2.5% confidence interval on the reduced χ^2 function.

Crystallography. Cell constants were determined by a least-squares fit to the setting parameters of 25 independent reflections measured on an Enraf-Nonius CAD4 four-circle diffractometer employing graphite-monochromated Mo Kα radiation (0.710 73 Å) and operating in the $\omega-2\theta$ scan mode. Data reduction and empirical absorption corrections (ψ scans) were performed with the WINGX[22] package. Structures were solved by the Patterson method with SHELXS-86[23] and refined by full-matrix least-squares analysis with SHELXL-97.[24] Drawings of molecules were produced with ORTEP-3.[25]

Crystal Data: $[ZnL^3Cl]ClO_4$, $C_{38}H_{48}Cl_2N_6O_4Zn$, $M = 789.09$ g mol^{-1}, monoclinic, $a = 35.268(9)$ Å, $b = 10.2200(10)$ Å, $c = 23.539(6)$ Å, $\beta = 118.69(2)°$, $U = 7443(3)$ Å^3, $T = 293$ K, space group $C2/c$ (No. 15), $Z = 8$, μ(Mo Kα) = 8.52 cm^{-1}, 6649 reflections measured, 6535 unique ($R_{int} = 0.2612$), which were used in all calculations, R1 = 0.0762 [for obsd data, $I > 2\sigma(I)$], wR2 = 0.2167 (all data).

Molecular Modeling. Molecular modeling of the Zn(II) complexes of L^3 and L^4 was performed with MOMEC97[26] using previously reported force-field parameters[27] to evaluate the likely solution conformations of these two molecules. A tetragonally elongated octahedral coordination environment about the metal ion was assumed in both cases by comparison to the reported structure[20] of a disubstituted bis(naphthalen-1-ylmethyl)amino derivative of L^1. Hence, complexes were modeled with four nitrogen donor atoms provided by tetradentate coordination of the macrocycle in the common *trans*-III N-based isomeric form[28] to give an equatorial N_4 plane with two solvent CH_3CN molecules bound in axial positions, completing the first-coordination sphere. Drawings of modeled structures were produced with RASMOL.[29]

Results

X-ray Crystallography. Crystals of $[ZnL^3Cl]ClO_4$ suitable for X-ray work were isolated by slow evaporation of an NMR sample in a 1:1 CD_3Cl/CD_3CN (v/v) solvent mixture, and

(21) Funston, A. M.; Ghiggino, K. P.; Grannas, M. J.; McFadyen, W. D.; Tregloan, P. A. *Dalton Trans.* **2003**, 3704.

(22) Farrugia, L. J. *J. Appl. Crystallogr.* **1999**, *32*, 8347.
(23) Sheldrick, G. M. *Acta Crystallogr., Sect. A* **1990**, *46*, 467.
(24) Sheldrick, G. M. *SHELXL-97: Program for Crystal Structure Determination*; University of Göttingen: Göttingen, Germany, 1997.
(25) Farrugia, L. J. *J. Appl. Crystallogr.* **1997**, *30*, 565.
(26) Comba, P., Hambley, T. W., Eds. *Molecular Modeling of Inorganic Compounds*; Wiley-VCH: NewYork, 1995.
(27) Bernhardt, P. V.; Comba, P. *Inorg. Chem.* **1992**, *31*, 2638.
(28) Bosnich, B.; Poon, C. K.; Tobe, M. L. *Inorg. Chem.* **1965**, *4*, 1102.
(29) Sayle, R. A.; Milner-White, E. J. *Trends Biochem. Sci.* **1995**, *20*, 374.

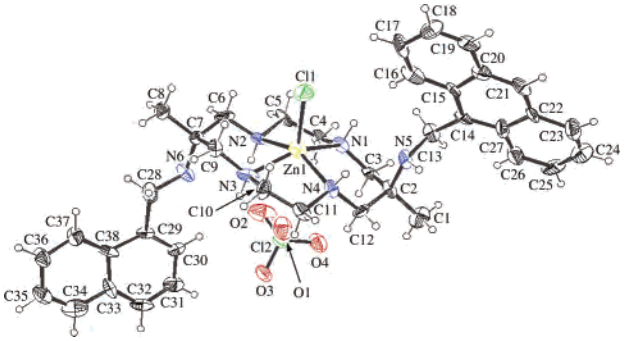

Figure 1. X-ray crystal structure of $[ZnL^3Cl]ClO_4$ (30% probability ellipsoids shown).

the resulting structure is shown in Figure 1. All atoms of the asymmetric ligand were located on general sites, with typical C−N and C−C alkyl bond lengths. Similarly, the naphthalene and anthracene ring systems, which are essentially planar, display C−C aromatic bond lengths that are typical. The coordination geometry of the complex cation is square-pyramidal, with four amine donors provided by the macrocycle, which encircles the metal ion, equatorially defining a basal plane and an axially coordinated chloro ligand at the apex. A perchlorate anion, loosely associated at the opposing axial site, completes the charge. The average of the Zn−N bond lengths is 2.12 Å, which is slightly elongated when compared to those of octahedral macrocyclic Zn(II) complexes.[20,30] However, as with previous square-pyramidal Zn(II) structures,[31] elongation of the Zn−N bonds is offset by a decrease in the axial Zn−Cl bond length, and concomitant displacement of the Zn(II) atom from the macrocyclic N_4 plane toward the coordinated chloro ligand, by 0.38 Å in the present case. Last, as with the previously reported structures of [Zn(II)cyclam]$^{2+}$ and its analogues,[30,31] the configuration of N donors adopted by the macrocycle is the energetically favored α-*trans*-III (RSSR) form, and the presence of the two bifurcated intramolecular hydrogen-bonding interactions between the pendant amino nitrogen lone pairs and protons of the coordinated secondary amines is apparent (N2−H2···N6 2.54 Å and N3−H3···N6 2.48 Å; N4−H4···N5 2.44 Å and N1−H1···N5 2.81 Å).

Steady-State Photophysics. Absorption, excitation, and emission spectra for the Zn(II) complex of L^3 have been previously reported,[16] and the corresponding spectra for the Zn(II) complex of L^4, as shown in Figure 2, were found to be essentially identical. In both cases, absorption spectra are effectively a superposition of the spectra of the naphthalene and anthracene chromophores, with two intense maxima at 223 and 254 nm attributable to the naphthalene and anthracene $S_0 \rightarrow S_3$ transitions, respectively. At slightly lower energy, the naphthalene $S_0 \rightarrow S_2$ and anthracene $S_0 \rightarrow S_1$ transitions were observed, the former as a shoulder at ca. 275 nm and the latter as a well-defined Franck−Condon vibrational progression with an origin at 385 nm and several peaks to higher energy separated by ca. 1420 cm^{-1}.

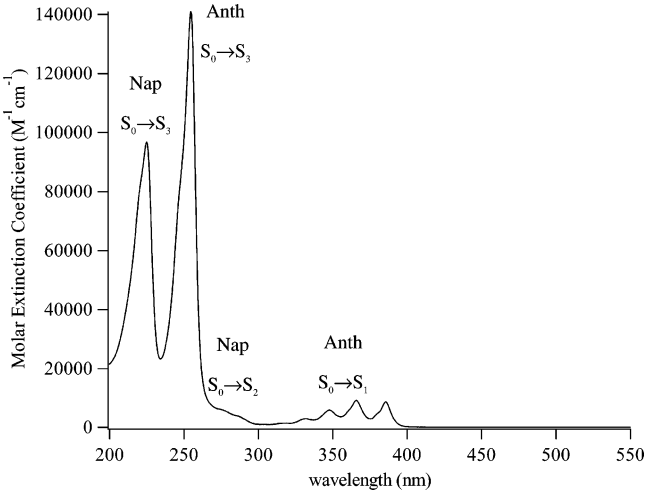

Figure 2. UV−visible absorption spectrum of $[ZnL^4]^{2+}$ in CH_3CN.

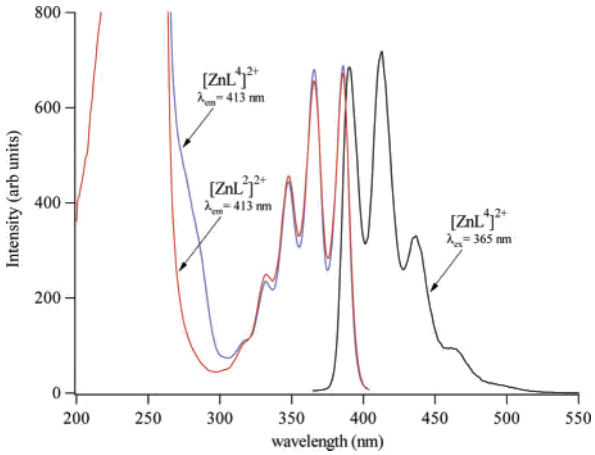

Figure 3. Emission and excitation spectra of $[ZnL^4]^{2+}$ and the corresponding excitation spectrum of the model $[ZnL^2]^{2+}$ complex.

The fluorescence excitation and emission spectra for the $[ZnL^3]^{2+}$ and $[ZnL^4]^{2+}$ complexes in CH_3CN are similarly almost identical, with those of the latter shown in Figure 3 together with the excitation spectra of the related model compound, $[ZnL^2]^{2+}$. A comparison of the fluorescence excitation spectra for $[ZnL^2]^{2+}$ and the bichromophoric $[ZnL^3]^{2+}$ and $[ZnL^4]^{2+}$ complexes, monitoring the anthracene emission at 413 nm, displays a new peak at 225 nm (data not shown) and a broad shoulder at ca. 280 nm in the latter two complexes. These new features correspond to absorption by the naphthalene chromophore and result in emission that is characteristic of the anthracene group. Excitation of the naphthalene chromophore in both the $[ZnL^3]^{2+}$ and $[ZnL^4]^{2+}$ complexes ($\lambda_{ex} = 275$ nm) yields emission spectra identical with those obtained upon direct excitation of the anthracene moiety at 390 nm, providing clear evidence of highly efficient EET operating in both of these complexes.

Time-Resolved Photophysics. Upon direct excitation of the anthracene $S_0 \rightarrow S_1$ transition at 390 nm, where absorption by the naphthalene chromophore is negligible, the fluorescence decays at 413 nm of both $[ZnL^3]^{2+}$ and $[ZnL^4]^{2+}$ were found to be biexponential, with fitting parameters as summarized in Table 1, which are in excellent agreement with those previously reported for the $[ZnL^2]^{2+}$

(30) Liang, X.; Weishaeupl, M.; Parkinson, J. A.; Parsons, S.; McGregor, P. A.; Sadler, P. J. *Chem.—Eur. J.* **2003**, *9*, 4709.
(31) Choi, K.-Y. *Polyhedron* **1997**, *16*, 2073.

Table 1. Fluorescence Decay and EET Rate Constant Parameters for $[ZnL^3]^{2+}$ and $[ZnL^4]^{2+}$ in CH_3CN at 298 K

complex	τ_1 (ns)	A_1 (%)	τ_2 (ns)	A_2 (%)	χ^2	$k_{EET(expt.)}$ ($\times 10^9$ s^{-1})	χ^2	Q_{EET} (%)	$k_{EET(calcd)}$ ($\times 10^9$ s^{-1})
$[ZnL^3]^{2+}$	2.37 ± 0.01	97 ± 0.8	7.41 ± 1.70	3.0 ± 1.5	1.43	0.92 ± 0.02	1.03	98.9	0.50
$[ZnL^4]^{2+}$	2.36 ± 0.04	93.0 ± 1.3	7.03 ± 0.68	7.0 ± 1.5	1.10	1.31 ± 0.01	1.20	98.4	0.73

model complex.[32] Alternately, fluorescence decay profiles, as shown in Figure 4, were collected for $[ZnL^3]^{2+}$ and $[ZnL^4]^{2+}$ using an excitation wavelength of 275 nm, corresponding to excitation into the naphthalene $S_0 \rightarrow S_2$ transition. The resulting emission was monitored at 413 nm, where fluorescence arises solely from the anthracene chromophore. The rise and decay of the experimental data were fit using a triple-exponential function incorporating the two decay components identified from direct measurements and a single-exponential rise term. Hence, experimental rate constants of EET in the $[ZnL^3]^{2+}$ and $[ZnL^4]^{2+}$ complexes were determined to be $(0.92 \pm 0.02) \times 10^9$ and $(1.31 \pm 0.01) \times 10^9$ s^{-1}, respectively.

The quantum efficiency of the EET reaction, Q, was estimated using the experimentally determined rate constants, k_{EET}, and the fluorescence lifetimes of 1-methylnaphthalene ($\tau = 97.0$ ns) and 2-methylnaphthalene ($\tau = 47.0$ ns) as the model donor chromophores.[33,34]

$$Q = k_{EET}/(k_{EET} + 1/\tau_D) \qquad (3)$$

Hence, EET efficiencies for the $[ZnL^3]^{2+}$ and $[ZnL^4]^{2+}$ complexes were 98.9% and 98.4%, respectively.

Molecular Modeling. Zn(II) complexes of L^3 and L^4 coordinated in the *trans*-III isomeric form can exist as two configurational diastereomers, namely, the α-*trans*-III or *β*-*trans*-III forms,[35] whereby the pendant nitrogen atom is on the same or opposite side of the macrocyclic N_4 plane as the adjacent coordinated secondary amine protons, respectively. As a result of this N-based isomerism, the pendant naphthalene and anthracene chromophores of $[ZnL^3]^{2+}$ and $[ZnL^4]^{2+}$ will both adopt either axial (α) or equatorial (*β*) dispositions with respect to their attached six-membered chelate rings, resulting in conformations that differ significantly in both the orientation and separation of the chromophores. However, recent results from Sadler et al. have shown that N-based isomerism in complexes with Zn(II) is labile, at least for the parent cyclam macrocycle, which undergoes rapid N-based isomerism within minutes of solubilizing an isomerically pure crystalline sample of known configuration.[30] Consequently, modeling of $[ZnL^3]^{2+}$ and $[ZnL^4]^{2+}$ was performed only for the α-*trans*-III N-based isomer because, on the basis of strain energies, it is this form that is most favorable as a result of the alternating chair and gauche conformations of the six- and five-membered chelate rings, respectively.[28] Furthermore, it is invariably this N-based isomeric form that is observed crystallographically for Zn(II) derivatives of cyclam,[30,36] the parent L^1 macrocycle,[37] and its functionalized derivatives.[20]

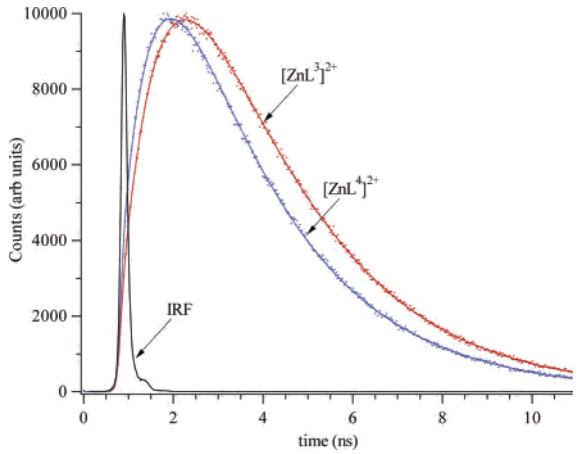

Figure 4. IRF and fluorescence decay profiles of $[ZnL^3]^{2+}$ and $[ZnL^4]^{2+}$ complexes in CH_3CN at 298 K. Experimental data (points) were fitted (solid line) to a triple-exponential rise-and-decay function (see text).

Modeling of the $[ZnL^3]^{2+}$ complex in the α-*trans*-III N-based isomeric form has been previously reported,[16] and an identical approach was utilized here. Briefly, for $[ZnL^3]^{2+}$, comprehensive conformational analysis of the ideal bond torsions for the appended 1-naphthyl chromophore with an axial (α) disposition located a total of 10 local minima. Similarly, for the 9-anthryl chromophore, which has local C_{2v} symmetry, there exist four local minima, which may be either syn or anti to the naphthalene. Hence, in combination, there exist a total of 80 2-fold degenerate combinations that were modeled. For $[ZnL^4]^{2+}$, less severe steric clashing interactions between the 2-naphthyl chromophore and the macrocycle result in a total of 15 local minima, which, in combination with the four minima for an axial (α) disposition of the 9-anthryl chromophore, yield a total of 120 combinations in the α-*trans*-III N-based isomeric form. The resulting global strain-energy-minimized structures for each complex are shown as insets in Figure 5.

Rate Calculations. The contribution to the overall rate constant of energy transfer via a Coulombic (dipole−dipole) mechanism can be evaluated using the Förster expression

$$k_{EET}^{dd} = \frac{9000 \ln(10)\kappa^2 \Phi_D J_{dd}}{128\pi^5 n^4 N_A \tau_D R^6} \qquad (4)$$

where κ^2 is an orientation factor, Φ_D the fluorescence quantum yield of the donor, n the refractive index of the medium, N_A Avogadro's number, τ_D the fluorescence lifetime of the donor in the absence of the acceptor, and R the donor−

(32) Moore, E. G.; Bernhardt, P. V.; Fürstenberg, A.; Riley, Mark, J.; Smith, T. A.; Vauthey, E. *J. Phys. Chem. A* **2005**, *109*, 3788.
(33) Cundall, R. B.; Pereira, L. C. *J. Chem. Soc., Faraday Trans. 2* **1972**, *68*, 1152.
(34) Meeus, F.; Van der Auweraer, M.; De Schryver, F. C. *J. Am. Chem. Soc.* **1980**, *102*, 4017.
(35) Bernhardt, P. V.; Jones, L. A.; Sharpe, P. C. *J. Chem. Soc., Dalton Trans.* **1997**, 1169.
(36) Alcock, N. W.; Berry, A.; Moore, P. *Acta Crystallogr. C* **1992**, *C48*, 16.
(37) Bernhardt, P. V.; Lawrance, G. A.; Maeder, M.; Rossignoli, M.; Hambley, T. W. *J. Chem. Soc., Dalton Trans.* **1991**, 1167.

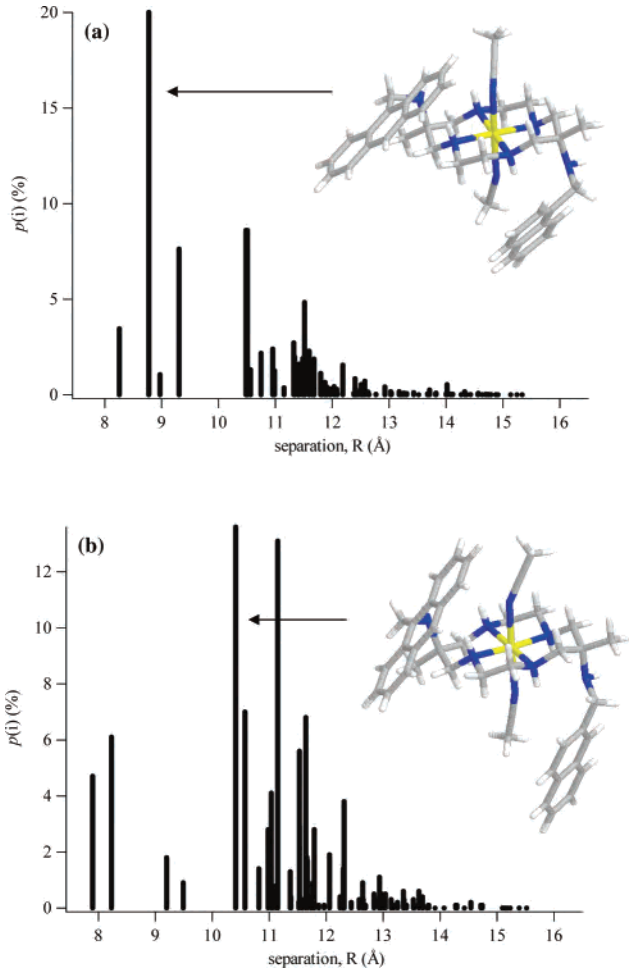

Figure 5. Conformational probability distributions for the α-*trans*-III N-based isomeric forms of the (a) $[Zn(L^3)(CH_3CN)_2]^{2+}$ and (b) $[Zn(L^4)(CH_3CN)_2]^{2+}$ complexes that were modeled. Insets: corresponding structures of the global strain-energy minimum.

acceptor separation. J_{dd} is the spectral overlap integral, defined as

$$J_{dd} = \int_0^{\infty} \frac{\bar{F}_D(\bar{\nu})\,\bar{\epsilon}_A(\bar{\nu})}{\bar{\nu}^4}\,d\bar{\nu} \qquad (5)$$

where $\bar{F}_D$ is the donor fluorescence spectrum normalized to the unit area, $\bar{\epsilon}_A$ is the acceptor's absorption spectrum, expressed by its molar extinction coefficient (M^{-1} cm^{-1}), and $\bar{\nu}$ is the wavenumber (cm^{-1}).

In the present case, the refractive index, n, of CH_3CN was taken to be 1.344, and literature values of 97.0 and 47.0 ns for the fluorescence lifetime, τ_D, of 1-methyl- and 2-methylnaphthalene as model donor chromophores were used.[33,34] Similarly, literature values[33,34] of 0.19 and 0.26 for the fluorescence quantum yields, Φ_D, of these model donor chromophores in a polar solvent were substituted where appropriate. The spectral overlap integral, J_{dd}, was determined experimentally to be $\sim 1.2 \times 10^{-15}$ M^{-1} cm^3 using the previously reported[38] normalized emission spectra of the parent L^1 macrocycle substituted with a single 1-naphthyl or 2-naphthyl chromophore, respectively, and the reported[19,32]

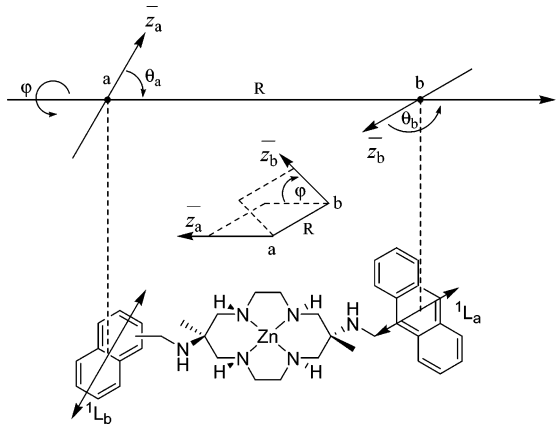

Figure 6. Dipole moment vectors for naphthalene, $\bar{z}_a$ (^1L_b transition, long axis polarized), and anthracene, $\bar{z}_b$ (^1L_a transition, short axis polarized), and hence the angles θ_a, θ_b, and φ used in eq 6 to determine κ^2.

absorption spectrum of $[ZnL^2]^{2+}$. The interchromophore separation, R, between the center of the naphthalene and anthracene ring systems was evaluated with the aid of the modeled structures for each strain-energy-minimized conformation. Last, the orientation factor, κ, was similarly individually determined for each strain-energy-minimized conformation using the modeled structures. Because the lowest-energy excited singlet states of the naphthalene and anthracene chromophores are known to be ^1L_b (long axis polarized) and ^1L_a (short axis polarized), respectively, and EET is normally assumed to occur between these states, the orientation factor may be readily determined using eq 6, where θ_a and θ_b are

$$\kappa = (2\cos\theta_a\cos\theta_b - \sin\theta_a\sin\theta_b\cos\varphi) \qquad (6)$$

the angles subtended by the dipole moment vector of donor and acceptor chromophores, respectively, on the interchromophore separation and φ is the torsional angle about the interdipole axis, as shown in Figure 6.[16] The results of these calculations for the global strain energy minimal conformations, shown as insets of Figure 5, gave k_{EET} values of 0.98×10^9 and 0.84×10^9 s^{-1} for $[ZnL^3]^{2+}$ and $[ZnL^4]^{2+}$, respectively. Importantly, to determine the overall calculated rate constant, the influence of the other conformers were evaluated by assuming that their contribution within the α-*trans*-III N-based isomeric form followed a Boltzmann distribution and that the rate of energy transfer was much faster than interconversion between conformers. From our modeling calculations, the barriers in terms of strain energy between conformational minima (which we approximate to the free energy) were on the order of 25−30 kJ mol^{-1}, yielding Eyring rate constants for conformer interconversion of 10^7−10^8 s^{-1}, at least an order of magnitude slower than the experimentally determined k_{EET}. The probability $p(i)$ of finding a conformer i is then given by[39]

$$p(i) = \exp\left(\frac{-E_i}{k_B T}\right) \Big/ \sum_j \exp\left(\frac{-E_j}{k_B T}\right) \qquad (7)$$

where E_i is the minimized strain energy of conformer i, k_B

(38) Bernhardt, P. V.; Moore, E. G.; Riley, M. J. *Inorg. Chem.* **2001**, *40*, 5799.

(39) Schael, F.; Rubin, M. B.; Speiser, S. *J. Photochem. Photobiol. A* **1998**, *115*, 99.

is the Boltzmann constant, and T was the temperature (298 K). The resulting probability distributions as a function of R, the interchromophore separation, are shown in Figure 5 for the $[ZnL^3]^{2+}$ and $[ZnL^4]^{2+}$ complexes, respectively. These were then used to calculate the relative contribution of each conformer to the overall rate of EET, which was evaluated by summation to be 0.50×10^9 and 0.73×10^9 s^{-1} for $[ZnL^3]^{2+}$ and $[ZnL^4]^{2+}$, respectively, as shown in Table 1.

Discussion

The preparations of the bichromophoric macrocycles described herein were quite straightforward, furnishing the desired products in excellent yield and in analytically pure form as confirmed by NMR and elemental analysis. Unfortunately, despite repeated attempts using both evaporative and diffusion techniques, with a variety of solvent systems, crystals of the asymmetrically disubstituted free ligands suitable for X-ray analysis were unable to be obtained. Rather, needlelike microcrystalline solids that were too small for X-ray work were consistently isolated.

The crystallization of $[ZnL^3Cl]ClO_4$ was informative and allows further aspects of the coordination tendency of Zn(II) with derivatives of the parent L^1 macrocycle to be explored. Most interestingly, the coordination geometry of the metal ion was square-based pyramidal, with the incorporation of a single chloride ligand in the apical position. This was somewhat dissimilar to the previously reported structure[20] of a disubstituted bis(naphthalen-1-ylmethyl)-amino derivative of L^1, where the metal ion coordination geometry was octahedral, with two solvent CH_3CN molecules in the axial positions and perchlorate counteranions on general sites in the unit cell. Importantly, chloride may be considered a more competitive donor than the weakly coordinating perchlorate anion, and square-pyramidal structures have been previously observed in its presence for other Zn(II) complexes of tetraaza macrocyclic ligands.[31,36] Indeed, this was the rationale for the use of $Zn(ClO_4)_2 \cdot 6H_2O$ as the Zn(II) salt in all photophysical measurements, such that the axial sites of the metal ion would be occupied by solvent molecules. Most importantly, in the present structure, and for a recently reported[40] Zn(II) complex of a functionalized L^1 derivative acting as a tetradentate ligand, the configuration of the macrocyclic amines was observed to be α-*trans*-III, which is the thermodynamically most favored form.

Electronic absorption spectra of the bichromophoric ligands and their corresponding Zn(II) complexes were found to be a simple superposition of the spectra for the individual components, with observed peaks in close agreement with the parent chromophores. The absence of any new bands is indicative of negligible ground-state interaction between the π-electron systems of the two chromophores. Upon excitation, the emission spectra of $[ZnL^3]^{2+}$ and $[ZnL^4]^{2+}$ are characteristic of the anthracene chromophore, regardless of the excitation wavelength. Moreover, the excitation spectrum monitored at 413 nm displayed new peaks that originate from absorption by the donor chromophore. These results clearly demonstrate the presence of an intramolecular energy-transfer pathway that quenches naphthalene fluorescence, the efficiency of which (ca. 99%) is comparable to that of previously reported systems.[7,12]

The fluorescence decay profiles of $[ZnL^3]^{2+}$ and $[ZnL^4]^{2+}$ upon direct excitation at 390 nm both required fitting by a biexponential decay function, contrary to the behavior previously reported[16] for $[ZnL^3]^{2+}$. This apparent disparity is likely due to the improved time resolution of the current experimental setup, coupled with a monochromatic detection wavelength, and the observed fluorescence behavior is consistent with that recently reported[32] for the model compound, $[ZnL^2]^{2+}$. In any case, a single component of this biexponential decay was found to be predominant (ca. 95%), with a lifetime of ~2.35 ns, which agrees well with that of the model complex, and may be assigned to the α-*trans*-III N-based isomeric form, which, based on modeling calculations, will be the dominant solution conformer. The time-resolved fluorescence profiles of the anthracene chromophore after excitation of the naphthalene chromophore at 285 nm have allowed the kinetics of the energy-transfer process to be evaluated. The contribution to the observed EET rate constant from a direct exchange (Dexter-type) mechanism may be safely neglected because of the large interchromophore separations (>8 Å), as indicated in Figure 5.

A comparison of the experimentally determined EET rate constant with those modeled via a direct Coulombic (Förster-type) interaction between the two chromophores indicated excellent agreement for both $[ZnL^3]^{2+}$ and $[ZnL^4]^{2+}$. Given the similarity of these results, it is with some confidence that the mechanism of EET in these complexes may be ascribed unequivocally to the Coulombic interaction. Hence, as previously reported for $[ZnL^3]^{2+}$, the through-bond and relayed mechanisms are apparently inoperative or inefficient in these complexes because of the inherent flexibility of the appended chromophores.

The slight differences between the observed EET rate constants for the 1-naphthyl- versus 2-naphthyl-substituted complexes are also in accord with the expectations of the Förster equation. Specifically, the larger fluorescence quantum yield, Φ_D, of the 2-naphthyl donor (0.26 compared to 0.19), in conjunction with its smaller fluorescence lifetime (47.0 ns compared to 97.0 ns), τ_D, would be expected to yield an enhanced EET rate constant, and this result is borne out by experiment. Interestingly, the enhancement is not as great as might be expected upon first consideration, although the reason for this becomes apparent upon inspection of Figure 5, where it can be seen that the anticipated enhancement is mitigated by a slight increase in the average interchromophore separation, R.

An important consideration has emerged from the molecular modeling studies performed for $[ZnL^3]^{2+}$ and $[ZnL^4]^{2+}$. First, it is of interest that if only the global strain-energy minima are used for subsequent EET rate calculations, the values obtained for k_{EET} are erroneous, predicting a faster rate constant for the 1-naphthyl-substituted complex, in contradiction with both the experimental values and the rates

(40) Bernhardt, P. V.; Creevey, N. L. *J. Chem. Soc., Dalton Trans.* **2004**, 914.

predicted using the more comprehensive approach. Hence, the possibility of multiple conformations, which are often neglected in studies of this type, must be considered, particularly for flexibly linked chromophores, to allow a closer quantitative examination of the role of the linker in facilitating EET.

Conclusions

The rate constant for EET in the Zn(II) complexes of two asymmetrically disubstituted macrocyclic bichromophores, $[ZnL^3]^{2+}$ and $[ZnL^4]^{2+}$, which differ only in the geometric isomerism of the donor, follows a simple Coulombic energy-transfer interaction between the naphthalene and anthracene chromophores. As with other flexibly linked systems, the relayed Coulombic and through-bond exchange-type interactions are minimal. As evidenced from the molecular modeling analysis, these complexes can exist in a wide variety of conformations through simple C−C or C−N bond rotation about the exocyclic amino groups. The importance of considering all of these conformations in interpreting the photophysical behavior was illustrated.

Acknowledgment. E.G.M. gratefully acknowledges financial support from the University of Queensland.

Supporting Information Available: Crystallographic data for $[ZnL^3Cl]ClO_4$ in CIF format. This material is available free of charge via the Internet at http://pubs.acs.org.

IC050396L